

Project 2

Transverse Loading Analysis of an Aircraft Wing

Carlos Anthony Natividad (917383302)

Huy Tran (918317542)

Michael Gunnarson (915204726)

March 5, 2023

Contents

1	Coordinate System, Project Geometry, and Loads	2
1.1	Coordinate System	2
1.2	Project Geometry	3
1.3	Loads	3
2	Methods	3
2.1	1-D Euler-Bernoulli Beam in Bending	3
2.2	Modulus-Weighted Centroid and Bending Stiffness in a Laminated Beam	6
3	Analysis and Results	8
3.1	Governing Equation Derivations	8
3.2	Young's Modulus for Each Orientation	8
3.3	Modulus Weighted Centroid and Bending Stiffness	9
3.4	Failure Analysis	10
3.5	Effect of Fuel Consumption on Wing	12
3.6	Additional Forces	12
4	Discussion	13
5	Team Member Contributions	13
6	Appendix	14
6.1	Material Properties	14
6.2	Code	15
6.3	Code Output	21
7	Citations	22

Abstract

As material science innovations have progressed throughout the last century, we have been updating our structures to increase stiffness, decrease weight, and create structural responses not possible previously. The wing is a major structural component that has been updated to utilize composites. In this study we explore the behavior of a wing under transverse loading due to lift. The x_1 axis is located along the length of the wing, x_2 points upwards at the root, and x_3 points towards the nose. To obtain the displacement u_2 , stress σ_1 , and subsequent point of failure we model the wing as a one-dimensional Euler-Bernoulli cantilever beam under a lifting transverse load. Due to the composite layering in the cross section of the wing, we must evaluate each layer's Young's Modulus to find the approximate, aggregate, or effective material properties. The most likely point of failure is at top layer of the root section with a stress of **145.6 MPa**. The wing will not fail under the given load. With a desired safety factor of 1.5, we can reduce the thickness of each composite layer to **0.819 mm** to find a new failure stress of **156.3 MPa**. This point of failure occurs in the same place as the original case. Further discussion is provided to allow for future work to account for loads that were neglected in this analysis.

1 Coordinate System, Project Geometry, and Loads

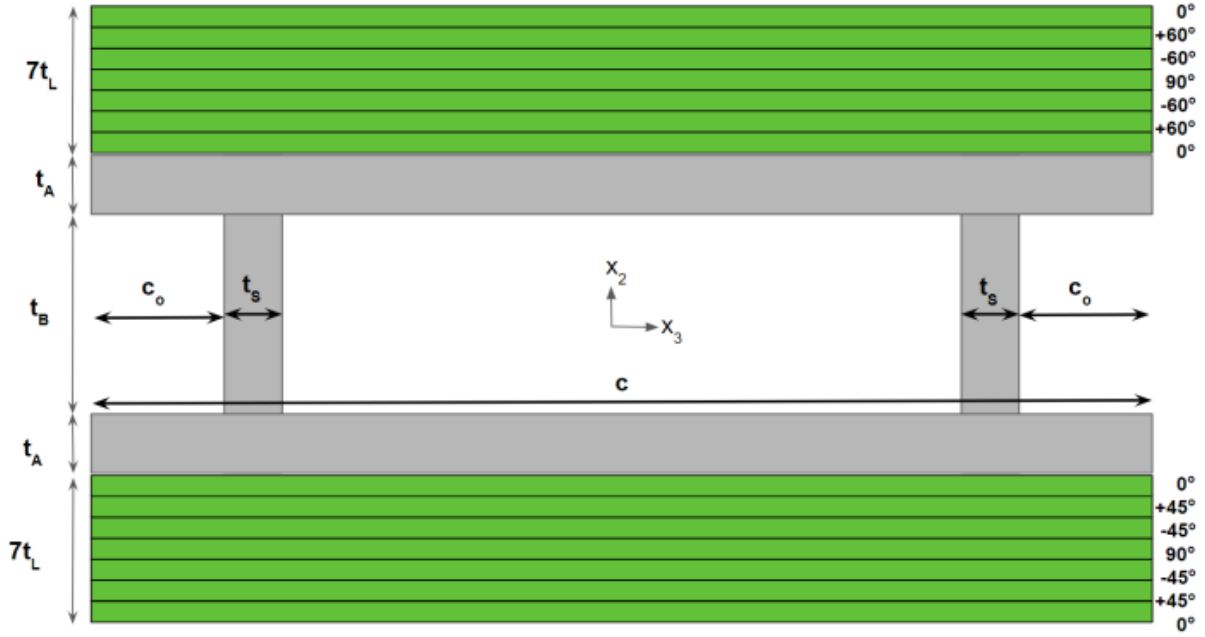


Figure 1

1.1 Coordinate System

In this problem, a wing is to be analyzed while being placed under a lifting load. The root of the wing will be fixed to a wall similar to how wings are attached to the fuselage on an aircraft. The x_1 direction runs parallel to the spar of the wing from the root to the tip. Bending inducted by a lifting force is applied vertically to the wing. To simplify the load, we align it to x_2 which points directly upwards. Based on the right-hand rule, this leaves x_3 directed along the fixed wall towards the leading edge of the wing. Similar to what is shown in the figure above, a temporary coordinate system will be positioned at the geometric center of the wing. Iterating through different thickness values for the wing, the center of the wing would continue to remain an equal distance from the top layer and the bottom layer, simplifying the calculations.

1.2 Project Geometry

The geometry of interest is part of a stiffener within the wing of the aircraft. Viewing the entity along the span of the wing, which is aligned with x_1 , the cross section of the wing can be simplified into two distinct parts. The first part is the aluminum skin of the wing which is composed of a box-beam placed horizontally between two C-beams. To strengthen the structure, Kelvar/epoxy composite is applied to the top and bottom of the aluminum skin in various layers along the x_2 direction. Each layer is modeled as a thin flat plate and with the fibers orientating differently between each layer, they have different properties between one another.

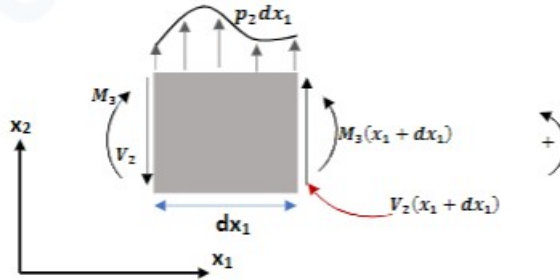
1.3 Loads

As mentioned previously, the lifting load is positioned along the x_2 axis and does not need to be projected on to x_1 or x_3 . The load distribution is described as $P_2(x_1) = -280.7x_1^2 + 3294x_1 + 58260$, which is a quadratic equation. Since there are no other loads or moments being experienced by the wing in any other direction, this situation turns into a purely bending problem without an axial load. Additionally, most of calculated results quantify displacements, moments, or stresses with respects to the x_2 direction.

2 Methods

2.1 1-D Euler-Bernoulli Beam in Bending

Since the given problem has lift as the only loading, we should model this wing as a one-dimensional Euler-Bernoulli cantilevered beam with transverse loading. Further considerations of this configuration might include drag and/or any kind of axial forces that might arise. The first step is to take an infinitesimal slice of the wing. This allows us to internally balance our forces, balance our moments, and derive the governing differential equations to solve for these internal forces. This internal loading assumes applied force to be upwards due to the fact that in aerospace contexts these are mostly lift forces.



Yuriy Honcharuk's rendition of the internal forces

After looking at an infinitesimal slice of the cross section, we can use a Taylor Series to approximate changes in shear and moments. The moment about axis 3 can be written as

$$M_3(x_1 + dx_1) = M_3(x_1) + \frac{dM_3}{dx_1}dx_1 + \dots$$

Ignoring higher order terms,

$$M_3(x_1 + dx_1) \cong M_3(x_1) + \frac{dM_3}{dx_1}dx_1$$

Using a Taylor Series, the shear in the direction of axis 2 can be written as

$$V_2(x_1 + dx_1) = V_2(x_1) + \frac{dV_2}{dx_1}dx_1 + \dots$$

Ignoring higher order terms,

$$V_2(x_1 + dx_1) \cong V_2(x_1) + \frac{dV_2}{dx_1}dx_1$$

Now that we have approximations for internal forces, we can use force and moment balances to generate the differential equation relationship. It is important to note that in comparison to the figure, dx_1 is small enough that P_2 is considered constant along the infinitesimally small domain. This means that $P_2 dx_1$ is a point force applied at the midpoint between x_1 and $x_1 + dx_1$. Looking at the 2 axis,

$$\sum F_2 = 0$$

$$-V_2(x_1) + P_2 + V_2 + \frac{dV_2}{dx_1} dx_1 = 0$$

$$\frac{dV_2}{dx_1} = -P_2$$

Looking at the 1 axis,

$$\sum F_1 = 0$$

Since there is no axial loading, $F_1 = 0$ Summing the moments,

$$\sum M_0 = 0$$

Where the subscript zero is the bottom left corner of the infinitesimal cube.

$$-M_3(x_1) + P_2 dx_1 * \frac{dx_1}{2} + (V_2 + \frac{dV_2}{dx_1} dx_1) dx_1 + M_3 + \frac{dM_3}{dx_1} dx_1$$

Assuming $dx_1^2 \approx 0$,

$$V_2 dx_1 + \frac{dM_3}{dx_1} dx_1 = 0$$

Recall that:

$$\frac{dM_3}{dx_1} = -V_2$$

Therefore we can relate the moment to the transverse lifting load:

$$\frac{d^2 M_3}{dx_1^2} = P_2(x_1)$$

Recall from the relation of bending stiffness to moment about axis 3,

$$M_3 = H_{33}^c \kappa_3$$

where $\kappa_3 = \frac{d^2 u_2}{dx_1^2}$ This allows us to get our governing equation for 1-D Euler-Bernoulli bending:

$$\frac{d^2}{dx_1^2} (H_{33}^c \frac{d^2 u_2}{dx_1^2}) = P_2(x_1)$$

Since we have modelled this wing as a cantilever beam the displacement and strain at the root are both zero. Because there is no applied load at the end of the beam, the moment and shear force at the tip are zero. This is summarized below:

$$\begin{cases} u_2(x_1 = 0) = 0 \\ \frac{du_2}{dx_1}(x_1 = 0) = 0 \\ M_3(x_1 = L) = 0 \\ V_2(x_1 = L) = 0 \end{cases}$$

With the boundary conditions known, the vertical displacement u_2 can be solved for. Recall the governing equation:

$$\frac{d^2}{dx_1^2} (H_{33}^c \frac{d^2 u_2}{dx_1^2}) = P_2(x_1)$$

Integrating with respect to x_1 gives us

$$\frac{d}{dx_1}(H_{33}^c \frac{d^2 u_2}{dx_1^2}) = \int P_2(x_1) dx_1 + C_1$$

Integrating again gives

$$H_{33}^c \frac{d^2 u_2}{dx_1^2} = \iint P_2(x_1) dx_1 + C_1 x_1 + C_2$$

Assuming H_{33}^c constant,

$$H_{33}^c \frac{du_2}{dx_1} = \iiint P_2(x_1) dx_1 + \frac{C_1 x_1^2}{2} + C_2 x_1 + C_3$$

Integrating and solving for u_2 gives you

$$u_2 = \frac{1}{H_{33}^c} \left[\iiint P_2(x_1) dx_1 + \frac{C_1 x_1^3}{6} + \frac{C_2 x_1^2}{2} + C_3 x_1 + C_4 \right]$$

To solve for u_2 , we must first know the load distribution to solve for the integration constants. The lift function is $P_2(x_1) = -280.7x_1^2 + 3294x_1 + 58260$ with units of Newtons per meter. We can then input the boundary conditions to solve for each integration constant. Starting with the root,

$$u_2(0) = 0 = \frac{1}{H_{33}^c} \left[\iiint P_2(x_1) dx_1 \Big|_{x_1=0} + \frac{C_1(0)^3}{6} + \frac{C_2(0)^2}{2} + C_3(0) + C_4 \right]$$

Many of the terms disappear, resulting in

$$C_4 = - \frac{1}{H_{33}^c} \iiint P_2(x_1) dx_1 \Big|_{x_1=0} = 0$$

We then solve for C_3 in a similar fashion such that

$$C_3 = - \frac{1}{H_{33}^c} \iint P_2(x_1) dx_1 \Big|_{x_1=0} = 0$$

To solve for C_1 and C_2 , we need to integrate the lift distribution so that we can evaluate them at nonzero values. We only need the first and second integrals of the lifting force to solve for the other constants, but the fourth integral is needed for the u_2 expression. Given generic coefficients of a quadratic equation and neglecting integration constants:

$$\begin{aligned} P_2 &= A_1 x^2 + A_2 x + A_3 \\ \int P_2 dx_1 &= \frac{A_1 x_1^3}{3} + \frac{A_2 x_1^2}{2} + A_3 x_1 \\ \iint P_2 dx_1 &= \frac{A_1 x_1^4}{12} + \frac{A_2 x_1^3}{6} + \frac{A_3 x_1^2}{2} \\ \iiint P_2 dx_1 &= \frac{A_1 x_1^5}{60} + \frac{A_2 x_1^4}{24} + \frac{A_3 x_1^3}{6} \\ \iiint P_2 dx_1 &= \frac{A_1 x_1^6}{360} + \frac{A_2 x_1^5}{120} + \frac{A_3 x_1^4}{24} \end{aligned}$$

Now using

$$V_2(L) = \frac{d}{dx_1}(H_{33}^c \frac{d^2 u_2}{dx_1^2}) = 0 = \int P_2(L) + C_1$$

Therefore,

$$C_1 = - \int P_2 dx_1 \Big|_{x_1=L}$$

Given $M_3(L) = 0$,

$$M_3(L) = H_{33}^c \frac{d^2 u_2}{dx_1^2}(L) = 0 = \iint P_2(L) + C_1 L + C_2$$

Therefore,

$$C_2 = - \iint P_2 dx_1 \Big|_{x_1=L} - C_1 L$$

This means that for our given loading conditions (evaluated at $L = 20.83$ meters)

$$C_1 = -1082524.10$$

$$C_2 = 9351688.36$$

And the equation for u_2 becomes:

$$u_2 = \frac{1}{H_{33}^c} \left[\iiint P_2(x_1) dx_1 - 180420.68x_1^3 + 4675844.18x_1^2 \right]$$

$$u_2 = \frac{1}{H_{33}^c} \left[-0.78x_1^6 + 27.45x_1^5 + 2427.50x_1^4 - 180420.68x_1^3 + 4675844.18x_1^2 \right]$$

These relationships allow us to find stresses and moments. These definitions are as follows:

$$\sigma_{1,i} = \frac{-E_i x_2 M_3}{H_{33}^c}$$

$$M_3 = \kappa_3 H_{33}^c$$

where

$$\kappa_3 = \frac{d^2 u_2}{dx_1^2}$$

For the stress equation, remember that x_2 is with reference to the modulus weighted centroid.

2.2 Modulus-Weighted Centroid and Bending Stiffness in a Laminated Beam

Looking along the span wise direction, the beam is laminated with multiple layers covering the skin of the wing. While the Young's modulus of the skin is indifferent to the axial direction, the value changes based on the referenced axis for the composite matrix. The primary stresses of interest in the x_1 and x_2 plane and the method required to compute the associating Young's modulus are listed below.

$$\begin{Bmatrix} \sigma_{11} \\ \sigma_{22} \\ \sigma_{12} \end{Bmatrix} = [Q] \begin{Bmatrix} \epsilon_{11} \\ \epsilon_{22} \\ \gamma_{12} \end{Bmatrix}$$

$$[Q] = \begin{bmatrix} \frac{E_{11}}{1-\nu_{12}\nu_{21}} & \frac{\nu_{21}E_{11}}{1-\nu_{12}\nu_{21}} & 0 \\ \frac{\nu_{12}E_{22}}{1-\nu_{12}\nu_{21}} & \frac{E_{22}}{1-\nu_{12}\nu_{21}} & 0 \\ 0 & 0 & G_{12} \end{bmatrix}$$

$$\nu_{21} = \nu_{12} \cdot \frac{E_{22}}{E_{11}}$$

Although each layer is associate with the same Kevlar/epoxy matrix, the orientation of the fibers within the matrix determines the Young's modulus with respects to the cross section of interest. When the fibers strands from the composite matrix are perpendicular to the displacement and moment of the wing, the stiffness is the highest since the fiber is fully being deformed, represented by 0° . However, the stiffness is much lower when the fibers are parallel to the moment since the strands cannot fully resistance the motion, represented by 90° . Using the variable β to represent the orientation of the fiber, we can determine the stiffness in the laminate layers through the following transformation and rotation matrices.

$$\begin{aligned}
\begin{bmatrix} \sigma_x \\ \sigma_y \\ \tau_{xy} \end{bmatrix} &= [\bar{Q}] \begin{bmatrix} \epsilon_x \\ \epsilon_y \\ \gamma_{xy} \end{bmatrix} \\
T &= \begin{bmatrix} \cos^2\beta & \sin^2\beta & 2\sin\beta\cos\beta \\ \sin^2\beta & \cos^2\beta & -2\sin\beta\cos\beta \\ -\sin\beta\cos\beta & \sin\beta\cos\beta & \cos^2\beta - \sin^2\beta \end{bmatrix} \\
R &= \begin{bmatrix} 1 & 0 & 0 \\ 0 & 1 & 0 \\ 0 & 0 & 2 \end{bmatrix} \\
\bar{Q} &= T^{-1} \cdot Q \cdot R \cdot T \cdot R^{-1}
\end{aligned}$$

With the effective Young's modulus of each layer determined in reference to the wingspan, it is possible to quantify where the neutral plane of the wing is. Using the modulus-weighted centriod method, we determine the location of the centroid based on the following equations.

$$\begin{aligned}
x_{2_c} &= \frac{\sum_i E_i A_i x_{2_i}}{\sum_i E_i A_i} \\
x_{3_c} &= \frac{\sum_i E_i A_i x_{3_i}}{\sum_i E_i A_i}
\end{aligned}$$

Note that due to the symmetry of the wing stiffener and laminated layers along the x_1 and x_2 plane, it is evident that x_{3_c} is zero with respects to the temporary coordinate system. To accumulate the effects from the entire wing through a single variable, we calculate the bending stiffness with respects to the centriod location calculated from the previous equations, measuring the wing's resistance to the moment generate from the lifting load.

$$H_{33}^c = \iint E x_2^2 dx_2 dx_3 = \frac{b}{3} \sum_{i=1}^n (E_{x_1 x_1})_i [(x_2)_{i+1}^3 - (x_2)_i^3]$$

3 Analysis and Results

3.1 Governing Equation Derivations

The relevant equations are derived in Section 2. The boundary conditions are also listed and briefly discussed in Section 2. Since there is no applied moment at the tip and no applied shear force, the moment and shear at the tip must be zero. At the root, a cantilever beam is defined by no displacement and no rotation. Thus all these boundary conditions are zero.

3.2 Young's Modulus for Each Orientation

Firstly, the material properties of the cross sections are outlined below.

Table 1: Material Properties

	7075-T73, A Basis	Kevlar/Epoxy
E_{11} [ksi]	10.7×10^3	11.0×10^3
E_{22} [ksi]	10.7×10^3	0.8×10^3
G_{12} [ksi]	4.0×10^3	0.3×10^3
ν_{12}	0.33	0.34
Tensile Yield Strength [ksi]	58.0	200
Compressive Yield Strength [ksi]	58.0	-34
Transverse Tensile Yield Strength [ksi]	—	4
Transverse Compressive Yield Strength [ksi]	—	-7.7

The axial Young's modulus for each layer of the laminate can be computed using the process outlined in the beginning of section 2.2. The results are shown below.

Table 2: Equivalent Young's Modulus

Kevlar/epoxy	Fiber Orientation (degree)	Young's Modulus (GPa)
Layer 1 (Bottom)	0	75.8
Layer 2	60	5.98
Layer 3	-60	5.98
Layer 4	90	5.52
Layer 5	-60	5.98
Layer 6	60	5.98
Layer 7	0	75.8
Layer 8	0	75.8
Layer 9	45	5.21
Layer 10	-45	5.21
Layer 11	90	5.52
Layer 12	-45	5.21
Layer 13	45	5.21
Layer 14 (Top)	0	75.8

3.3 Modulus Weighted Centroid and Bending Stiffness

Using these equivalent axial stiffness for each layer, the modulus weighted centroid is **0.270 mm** below the centerline of the cross section. From this reference, the bending stiffness can be calculated using the method at the end of section 2.2. For this cross section, the bending stiffness (H_{33}^c) is **$2.619 \times 10^9 N/m^2$** . Now that the bending stiffness is known, the displacement and moment can be known.

$$u_2 = \frac{1}{2.619 \times 10^9} (-0.78x_1^6 + 27.45x_1^5 + 2427.50x_1^4 - 180420.68x_1^3 + 4675844.18x_1^2) \text{ [m]}$$

$$M_3 = -23.4x_1^4 + 549x_1^3 + 29130x_1^2 - 1082524.1x_1 + 9351688.4 \text{ [N} \cdot \text{m]}$$

Because there is no net axial stress, $\sigma_1(x_1) = 0$. The bending moment and displacement for this lift distribution and thickness are shown below.

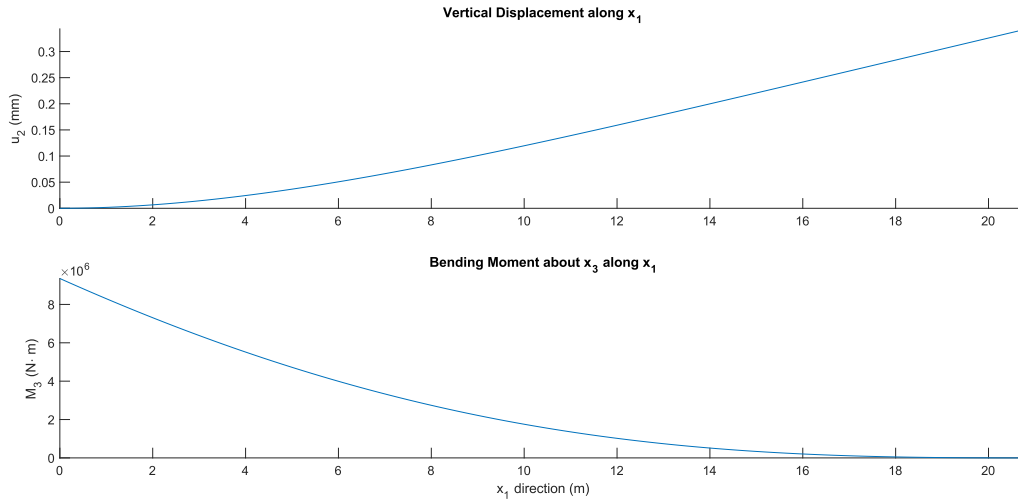


Figure 2: Pure Bending Effects along Wingspan

3.4 Failure Analysis

Because the cross section is uniform throughout the wing, the location of maximum stress is in the cross section at the root of the wing. Here, the bending moment is the greatest. The stress distribution for the root cross section is shown below.

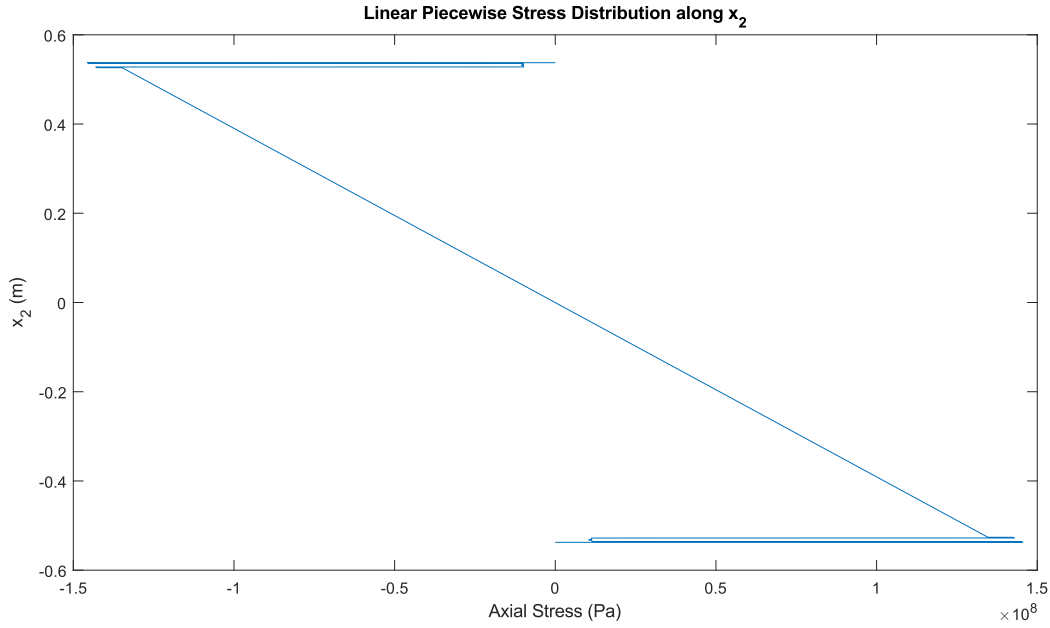


Figure 3: Stress Distribution along Wing Cross Section

The stress distribution in the laminate is difficult to see on the full scale, so below are some plots to only show the distribution within the laminate.

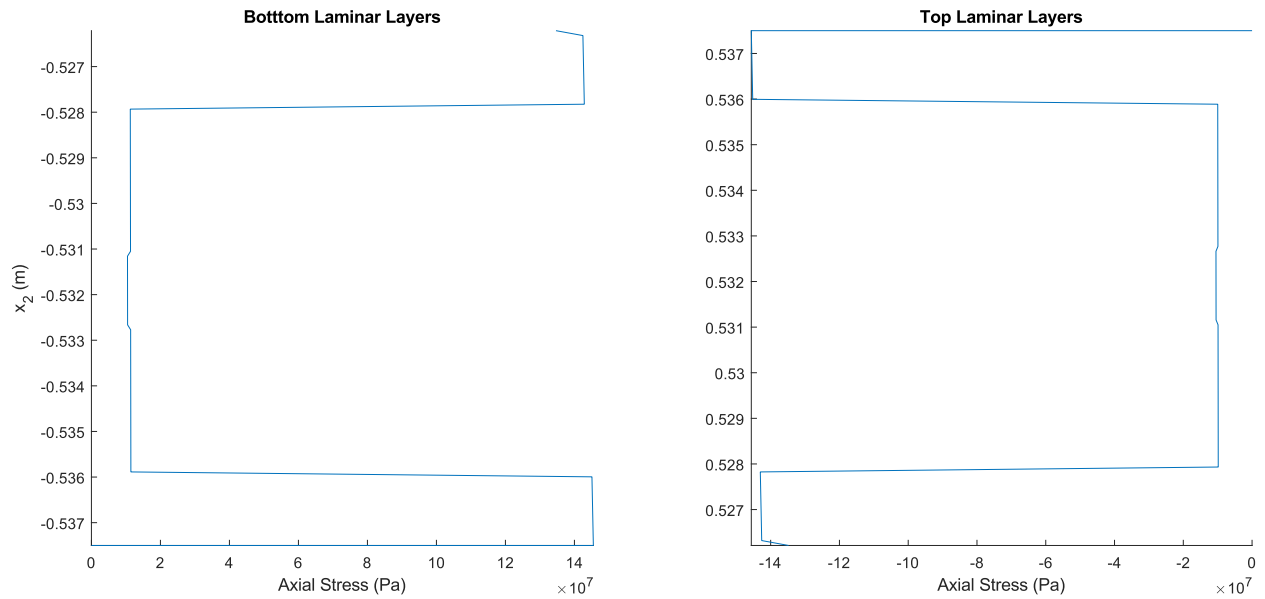


Figure 4: Stress Distribution at the composite layers

The maximum stress for each homogeneous layer will be at the outermost location from the midline. These stresses are tabulated below for the root section. The factor of safety is calculated based on whether the layer is in tension or compression and whether or not the composite layers are oriented in the direction of loading. For composite layers that are at an angle from the direction of loading, the transverse yield strengths are used to calculate the factor of safety.

Table 3: Max Stress in Each Layer of the Root Section, $t_{Lp} = 1.6 \text{ mm}$

	Fiber Orientation (degree)	Axial Stress (MPa)	Factor of Safety
Kevlar/epoxy Layer 1 (Bottom)	0	145.5	9.478
Kevlar/epoxy Layer 2	60	11.4	2.412
Kevlar/epoxy Layer 3	-60	11.4	2.419
Kevlar/epoxy Layer 4	90	10.5	2.63
Kevlar/epoxy Layer 5	-60	11.3	2.433
Kevlar/epoxy Layer 6	60	11.3	2.441
Kevlar/epoxy Layer 7	0	142.9	9.651
Aluminum Skin	—	134.7	2.969
Aluminum Skin	—	134.8	2.966
Kevlar/epoxy Layer 8	0	143	1.639
Kevlar/epoxy Layer 9	45	9.86	5.382
Kevlar/epoxy Layer 10	-45	9.89	5.366
Kevlar/epoxy Layer 11	90	10.5	5.058
Kevlar/epoxy Layer 12	-45	9.95	5.334
Kevlar/epoxy Layer 13	45	9.98	5.318
Kevlar/epoxy Layer 14 (Top)	0	145.6	1.61

For this thickness, none of the layers fail or have a factory of safety below 1.5. This means we can reduce the thickness of the layers to save weight while maintaining a factor of safety of 1.5. Recognizing that the top layer is the first point of failure, we will find a minimum thickness for the laminate such that the factor of safety is only 1.5. This is done to reduce the weight of the wing while allowing ample room to allow the wing to sustain higher loads. An iterative method was used to find a minimum thickness of **0.819 mm**. The stresses for this new wing section are shown below.

Table 4: Stress Distribution of the Root Section, $t_{Lp} = 0.819 \text{ mm}$

	Fiber Orientation (degree)	Axial Stress (MPa)	Factor of Safety
Kevlar/epoxy Layer 1 (Bottom)	0	156.2	8.828
Kevlar/epoxy Layer 2	60	12.3	2.243
Kevlar/epoxy Layer 3	-60	12.3	2.246
Kevlar/epoxy Layer 4	90	11.3	2.439
Kevlar/epoxy Layer 5	-60	12.2	2.253
Kevlar/epoxy Layer 6	60	12.2	2.257
Kevlar/epoxy Layer 7	0	154.8	8.911
Aluminum Skin	—	146.1	2.737
Aluminum Skin	—	146.2	2.736
Kevlar/epoxy Layer 8	0	154.8	1.514
Kevlar/epoxy Layer 9	45	10.7	4.979
Kevlar/epoxy Layer 10	-45	10.7	4.971
Kevlar/epoxy Layer 11	90	11.3	4.693
Kevlar/epoxy Layer 12	-45	10.7	4.956
Kevlar/epoxy Layer 13	45	10.7	4.948
Kevlar/epoxy Layer 14 (Top)	0	156.3	1.5

This new thickness is is about half of the original value. This means that the laminate is about half the original weight. Weight reduction in aircraft often comes with a snowball effect. This reduction in weight will also result in a reduction in the wing loading. This means that the thickness can be further reduced, but will eventually converge onto a smaller value.

3.5 Effect of Fuel Consumption on Wing

Over the course of a flight, the weight decreases due to fuel consumption. This affects aircraft speed and angle of attack, but since fuel is often stored in hollow wings, it also affects the applied forces on the wing in the 2 direction.

Since weight was not considered in this study up until this point, additional exploration should be briefly discussed. In looking at our original model used to derive our governing equations, we could easily place an applied weight $w dx_1$ along the vertical center line of our infinitesimally small slice. This assumes that w is in units of Newtons per meter and describes the weight of the wing.

Since w and P_2 act along the same line and create mathematically similar forces and moments, the model could be updated by simply defining a new load function (or forcing function) and substituting this load into all subsequent general derivations for u_2 and the like:

$$P^* \equiv P_2 - w$$

It is important to note that the boundary conditions would not change but the constants of integration would, meaning that a re-derivation of the constants of integration would be necessary, as well as re-calculating the integrals for the forcing function. For the general case, u_2 , for example, could be described by

$$u_2 = \frac{1}{H_{33}^c} \left[\iiint P^*(x_1) dx_1 + \frac{C_1 x_1^3}{6} + \frac{C_2 x_1^2}{2} + C_3 x_1 + C_4 \right]$$

Over the course of a flight, $w(x_1, t)$ decreases with time. This means that the resultant load function will increase with time, increasing displacement, moment, shear, and stress within the wing, assuming all else constant. In actuality, a decrease in weight means that steady and level flight conditions change, and angle of attack or speed change to match the new stable flight condition. To be clear, as weight decreases, the pilot will change flight conditions to decrease lift to match a decrease in weight. Since the wings lift the weight of the entire plane and not just their own weight, the moment, shear, and stresses within the wing will still increase with time. Additional studies will be needed to explore the exact nature of this relationship, but a 1.5 safety factor would need to be applied to the worst case scenario weight and lift distributions to make accurate design decisions.

3.6 Additional Forces

This study does not analyze the affects of drag on a wing. This additional loading force would require the cantilevered beam to be in 2 dimensions, bending about the 2 and 3 axes respectively. In addition, the effects of weight are not considered either, though as shown above are a simple extension of our discussion, assuming constant with time. Similarly to weight, Drag and Thrust operate in the same direction and would be derived in a similar manner. There are likely no axial forces to be accounted for unless there is a winglet at significantly steep angle on the wing tip. The pressure differential across the wing would normally create lift, but since winglets are angled this force would be directed towards the fuselage. This force is likely minimal, but could theoretically cause different boundary conditions, like a cantilever beam with applied moment and shear force at its tip to model the affect of the winglet. Another force that was neglected is the torsional moment caused by wings at angles of attack. Because most of the lift is generated in the first half of the chordwise section, a positive pitching moment is present. Because this is not a circular cross section and it is unlikely for the twist rate to be constant, there are many complexities that are not being accounted for by ignoring torsion. Beyond this, the next most likely force would be destructive high-speed impacts. Though beyond the scope of this class, it is vital that a plane's structure and engine survive collisions with a bird.

4 Discussion

The analysis found that the current design has a larger factor of safety than desired. This motivated a calculation of the minimum lamina thickness required in order to satisfy the factor of safety requirement, resulting in half the original thickness. This reduction in thickness will also result in a reduction in the weight of the aircraft. While it may be beneficial to find the optimal thickness for each layer, the one dimensional analysis is too limited to reach a reasonable result. Although already mentioned in sections 3.5 and 3.6, it is also important to discuss the pitfalls of this model. This model does not address the weight of the wing, as discussed previously, fuel weight within wing, the transverse force of drag, as well as the load factor during maneuvers that are not steady and level flight. Most importantly, we have also neglected any torsional forces caused by the chordwise pressure distribution. There are many ways that the design of the wing can be improved. One of them is find ways to minimize the bending moment by altering the lift distribution. This can be done by tapering the wing, resulting in more of the lift being generated closer to the root. Another option is to consider that for the same root bending moment, a bell shaped lift distribution can result in the highest span efficiency. Ultimately, tapering the wing will allow for material to be removed in the outer sections where it is not needed and added to the root where it is. In order to maximize the bending stiffness without adding more weight, more material should be placed further away from the modulus weighted centroid in order to allow for a greater lever arm to counteract the bending moment. Thicker airfoils are typically used at the root for both structural and aerodynamic gain.

5 Team Member Contributions

Carlos Anthony Natividad: Code for calculating x_{2c} , H_{33}^c , and t_{Lf} . Wrote section 3.4. Discussion. Final Review of Report.

Huy Tran: Coordinate System, Project Geometry, and Loads. Modulus-Weighted Centroid and Bending Stiffness in a Laminated Beam section. Final Review of Report and Formatting of Tables and Graphs.

Michael Gunnarson: derived and wrote the methods section 1-D Euler-Bernoulli Beam in Bending. Wrote script to solve for u_2 , σ_1 , M_3 , K_3 , and integration constants in terms of H_{33} and E . Wrote sections 3.1, 3.5, and 3.6

6 Appendix

6.1 Material Properties

Table 3.7.6.0(g₂). Design Mechanical and Physical Properties of 7075 Aluminum Alloy Extrusion—Continued

Specification	AMS-QQ-A-200/11													
Form	Extrusion (rod, bars, and shapes)													
Temper	T73 ^a , T73510, T73511													
Cross-Sectional Area, in. ²	≤20		≤25								≤20		>20, ≤32	
Thickness, in. ^b	0.062-0.249		0.250-0.499		0.500-0.749		0.750-1.499		1.500-2.999		3.000-4.499		3.000-4.499	
Basis	A	B	A	B	A	B	A	B	A	B	A	B	A	B
Mechanical Properties:														
F_{pu} , ksi:														
\bar{L}	68 ^c	72	70 ^d	74	70 ^d	73	70 ^d	73	69 ^d	74	68 ^c	71	65 ^e	70
LT	66	70	68	72	67	70	66	69	62	67	58	61	56	60
F_{pu} , ksi:														
\bar{L}	58	61	60	63	60	63	60	63	59 ^d	65	57 ^c	62	55 ^e	60
LT	56	59	57	60	57	60	56	58	51	56	46	50	44	48
F_{cu} , ksi:														
\bar{L}	58	61	60	63	60	63	60	63	59	65	57	62	55	60
LT	59	62	60	63	60	63	58	61	54	59	49	53	47	51
F_{pu} , ksi:														
\bar{L}	37	39	38	40	38	39	38	39	37	40	37	38	35	38
F_{pu} , ksi:														
(e/D = 1.5)	101	107	104	110	103	108	103	107	99	106	95	99	91	98
(e/D = 2.0)	129	137	133	141	133	139	132	138	128	138	124	130	119	128
F_{pu} , ksi:														
(e/D = 1.5)	82	86	84	89	84	88	83	87	79	87	72	79	70	76
(e/D = 2.0)	97	102	100	105	100	105	98	103	93	103	86	94	83	91
e, percent (S-basis):														
\bar{L}	7	...	8	...	8	...	8	...	8	...	7	...	7	...
E , 10 ³ ksi	10.4													
E_c , 10 ³ ksi	10.7													
G , 10 ³ ksi	4.0													
μ	0.33													
Physical Properties:														
ω , lb/in. ³	0.101													
C, K, and α	See Figure 3.7.6.0													

Table 5: 7075-T73 Material Properties

Material	AS4/epoxy (Vf = 0.62)	T300/epoxy (Vf = 0.62)	Kevlar/epoxy (Vf = 0.55)	S2 glass/epoxy (Vf = 0.60)
Density (lb/in ³)	0.055	0.056	0.05	0.072
Ply thickness (in.)	0.005	0.005	0.005	0.009
E11 (Msi)	21.5	19.2	11.0	6.31
E22 (Msi)	1.46	1.56	0.8	1.67
v12	0.30	0.24	0.34	0.27
G12 (Msi)	0.81	0.82	0.3	0.50
Axial tensile strength (ksi)	310	219	200	250
Transverse tensile strength (ksi)	7.75	6.3	4.0	6.0
Axial compressive strength (ksi)	-184	-226	-34	-120
Transverse compressive strength (ksi)	-24.4	-28.9	-7.70	-17.1
Axial tensile max strain	0.0140	0.0124	0.0185	0.0295
Axial compressive max strain	-0.010	-0.010	-0.0031	-0.0173

Table 6: AS4 material properties

6.2 Code

```
clc
clear
close all
format compact
format shortg

%% 1| Displacements, Forces, and Moments derivation
A1 = -280.7;
A2 = 3294;
A3 = 58260;

% ignoring integration constants
P2 = @(x) A1*x.^2 + A2*x + A3;
IP2 = @(x) A1/3*x.^3 + A2/2*x.^2 + A3*x;
IIP2 = @(x) A1/12*x.^4 + A2/6*x.^3 + A3/2*x.^2;
IIIP2 = @(x) A1/60*x.^5 + A2/24*x.^4 + A3/6*x.^3;
IIIP2 = @(x) A1/360*x.^6 + A2/120*x.^5 + A3/24*x.^4;

length = 20.83; % meters

C1 = -IP2(length);
C2 = -IIP2(length) - length*C1;

u2 = @(x1,H33) 1/H33 * (IIIP2(x1) + C1/6 * x1.^3 + C2/2 * x1.^2);
ddu2 = @(x1,H33) 1/H33 * (IIP2(x1) + C1*x1 + C2); % second derivative of u2
K3 = ddu2

M3 = @(x1,H33) H33* K3(x1,H33);
Sigma1 = @(x1,x2,E,H33) - E .* x2 * M3(x1,H33)/H33;

%% 2| H33c Calculation

L = 20.83; % m
c = 254e-2; % m
%c_0 =
t_B = 105e-2; % m
t_A = 1.3e-3; % m
t_S = 15e-2; % m
t_Lp = 1.6e-3; % m
% t_Lf =

% Kevlar/Epoxy
E_11kevlarepoxy = 11e6 * 6894.75729; % Pa
E_22kevlarepoxy = .8e6 * 6894.75729; % Pa
G_12kevlarepoxy = .3e6 * 6894.75729; % Pa
nu_12kevlarepoxy = 0.34;

E_11tykevlarepoxy = 200e3 * 6894.75729; % Pa
E_22tykevlarepoxy = 4.0e3 * 6894.75729; % Pa
```



```

E_11cykevlar epoxy = -34e3 * 6894.75729; % Pa
E_22cykevlar epoxy = -7.70e3 * 6894.75729; % Pa
% 7075-T73
E_11alum = 10.4e6 * 6894.75729; % Pa
E_22alum = 10.4e6 * 6894.75729; % Pa
G_12alum = 4e6 * 6894.75729; % Pa
nu_12alum = 0.33;

E_11tyalum = 58e3 * 6894.75729; % Pa
E_11cyalum = 58e3 * 6894.75729; % Pa

thickness = [repmat(t_Lp,7,1);t_A;t_B;t_A;repmat(t_Lp,7,1)];
chord = ones(17,1)*c; chord(9) = t_S*2;
theta = [0;45;-45;90;-45;45;0;0;0;0;60;-60;90;-60;60;0]*pi/180;
E_11 = [repmat(E_11kevlar epoxy,7,1);repmat(E_11alum,3,1);repmat(E_11kevlar epoxy,7,1)];
E_22 = [repmat(E_22kevlar epoxy,7,1);repmat(E_11alum,3,1);repmat(E_22kevlar epoxy,7,1)];
E_11ty = [repmat(E_11tykevlar epoxy,7,1);repmat(E_11tyalum,3,1);repmat(E_11tykevlar epoxy,7,1)];
E_22ty = [repmat(E_22tykevlar epoxy,7,1);repmat(E_11tyalum,3,1);repmat(E_22tykevlar epoxy,7,1)];
E_11cy = [repmat(E_11cykevlar epoxy,7,1);repmat(E_11cyalum,3,1);repmat(E_11cykevlar epoxy,7,1)];
E_22cy = [repmat(E_22cykevlar epoxy,7,1);repmat(E_11cyalum,3,1);repmat(E_22cykevlar epoxy,7,1)];
G_12 = [repmat(G_12kevlar epoxy,7,1);repmat(G_12alum,3,1);repmat(G_12kevlar epoxy,7,1)];
nu_12 = [repmat(nu_12kevlar epoxy,7,1);repmat(nu_12alum,3,1);repmat(nu_12kevlar epoxy,7,1)];

[coords,E_11e,x_2c,H_33c] = sandwich(thickness,chord,theta,E_11,E_22,G_12,nu_12);

%% 3| Displacement and Moment Plots
% [Reminder:]
%  $u_2 = @ (x_1, H_{33}) \frac{1}{H_{33}} * (IIII L(x_1) + C1/6 * x_1.^3 + C2/2 * x_1.^2);$ 
%  $M_3 = @ (x_1, H_{33}) H_{33} * K_3(x_1, H_{33});$ 
%  $\sigma_1 = @ (x_1, x_2, E, H_{33}) - E * x_2 * M_3(x_1)/H_{33};$ 

x_1 = linspace(0,L,101);
cfigure([.5,.5])
subplot(2,1,1)
hold on
plot(x_1,u2(x_1,H_33c))
axis tight
ylabel("u_2 (mm)");
title("Vertical Displacement along x_1");

subplot(2,1,2)
hold on
plot(x_1,M3(x_1,H_33c))
axis tight
xlabel("x_1 direction (m)");
ylabel("M_3 (N\cdot m)");
title("Bending Moment about x_3 along x_1");

%% 4| Failure Analysis
% [Reminder:]
%  $\sigma_1 = @ (x_1, x_2, E, H_{33}) - E * x_2 * M_3(x_1)/H_{33};$ 
[val,index] = max(M3(x_1,H_33c));
% x2 =
t_total = sum(thickness);

```

```

x_2 = linspace(-t_total/2,t_total/2,10001)';
E_11layer = E_11e(discretize(x_2,coords));
cfigure([.4,.5])
plot([0;Sigma1(x_1(index),x_2-x_2c,E_11layer,H_33c);0],[x_2(1);x_2;x_2(end)]);
xlabel("Axial Stress (Pa)");
ylabel("x_2 (m)");
title("Linear Piecewise Stress Distribution along x_2");

cfigure([.5,.5])
subplot(1,2,1)
hold on
plot([0;Sigma1(x_1(index),x_2(1:106)-x_2c,E_11layer(1:106),H_33c)], [x_2(1);x_2(1:106)])
axis tight
ylabel("x_2 (m)");
xlabel("Axial Stress (Pa)");
title("Botttom Laminar Layers");

subplot(1,2,2)
hold on
plot([Sigma1(x_1(index),x_2(9896:end)-x_2c,E_11layer(9896:end),H_33c);0],[x_2(9896:end);x_2(end)])
axis tight
xlabel("Axial Stress (Pa)");
title("Top Laminar Layers");

% recognize that max stress will be at the outer layer of the layer:
% check bottom layers
for i = 1:8
    Sigma = Sigma1(x_1(index),coords(i)-x_2c,E_11e(i),H_33c);
    if Sigma > 0
        mode = '(T)';
        if theta(i) == 0
            Ey = E_11ty(i);
        else
            Ey = E_22ty(i);
        end
    else
        mode = '(C)';
        if theta(i) == 0
            Ey = E_11cy(i);
        else
            Ey = E_22cy(i);
        end
    end

    if abs(Sigma) > abs(Ey)
        fprintf(' [FAILED] ')
    else
        fprintf(' [n_f = %.3f] ',abs(Ey/Sigma))
    end

    fprintf('Layer %g = %.3e Pa %s\n',i,Sigma,mode)
end
% check top layers
for i = 11:18

```

```

Sigma = Sigma1(x_1(index),coords(i)-x_2c,E_11e(i-1),H_33c);
if Sigma > 0
    mode = '(T)';
    if theta(i-1) == 0
        Ey = E_11ty(i-1);
    else
        Ey = E_22ty(i-1);
    end
else
    mode = '(C)';
    if theta(i-1) == 0
        Ey = E_11cy(i-1);
    else
        Ey = E_22cy(i-1);
    end
end

if abs(Sigma) > abs(Ey)
    fprintf(' [FAILED] ')
else
    fprintf(' [n_f = %.3f] ',abs(Ey/Sigma))
end
fprintf('Layer %g = %.3e Pa %s\n',i-1,abs(Sigma),mode)
end

% now to get least thickness
t_Lf = [t_Lp,.99*t_Lp];
n_f = 1.5;

r=1;

%
while r > 1e-6
    thickness = [repmat(t_Lf(1),7,1);t_A;t_B;t_A;repmat(t_Lf(1),7,1)];
    [coords,E_11e,x_2c,H_33c] = sandwich(thickness,chord,theta,E_11,E_22,G_12,nu_12);
    % only check the top layer at the root (lowest safety factor)
    SigmaOld = Sigma1(x_1(1),coords(18)-x_2c,E_11e(17),H_33c);
    n_fOld = abs(E_11cykevlar epoxy/SigmaOld);

    thickness = [repmat(t_Lf(2),7,1);t_A;t_B;t_A;repmat(t_Lf(2),7,1)];
    [coords,E_11e,x_2c,H_33c] = sandwich(thickness,chord,theta,E_11,E_22,G_12,nu_12);
    % only check the top layer at the root (lowest safety factor)
    SigmaNew = Sigma1(x_1(1),coords(18)-x_2c,E_11e(17),H_33c);
    n_fNew = abs(E_11cykevlar epoxy/SigmaNew);

    cor = -(n_fNew-n_f)*(t_Lf(2)-t_Lf(1))/(n_fNew-n_fOld);
    t_Lf = [t_Lf(2),t_Lf(2)+cor];

    % residual calc

    thickness = [repmat(t_Lf(2),7,1);t_A;t_B;t_A;repmat(t_Lf(2),7,1)];
    [coords,E_11e,x_2c,H_33c] = sandwich(thickness,chord,theta,E_11,E_22,G_12,nu_12);
    SigmaNew = Sigma1(x_1(1),coords(18)-x_2c,E_11e(17),H_33c);
    r = abs(n_f-abs(E_11cykevlar epoxy/SigmaNew));

```

```

end

% check the solution
fprintf('\n\n[Reduced Thickness = %.3f mm]\n',t_Lf(2)*1e3)
% check bottom layers
for i = 1:8
    Sigma = Sigma1(x_1(index),coords(i)-x_2c,E_11e(i),H_33c);
    if Sigma > 0
        mode = '(T)';
        if theta(i) == 0
            Ey = E_11ty(i);
        else
            Ey = E_22ty(i);
        end
    else
        mode = '(C)';
        if theta(i) == 0
            Ey = E_11cy(i);
        else
            Ey = E_22cy(i);
        end
    end

    if abs(Sigma) > abs(Ey)
        fprintf('[FAILED]')
    else
        fprintf('[n_f = %.3f] ',abs(Ey/Sigma))
    end

    fprintf('Layer %g = %.3e Pa %s\n',i,Sigma,mode)
end
% check top layers
for i = 11:18
    Sigma = Sigma1(x_1(index),coords(i)-x_2c,E_11e(i-1),H_33c);
    if Sigma > 0
        mode = '(T)';
        if theta(i-1) == 0
            Ey = E_11ty(i-1);
        else
            Ey = E_22ty(i-1);
        end
    else
        mode = '(C)';
        if theta(i-1) == 0
            Ey = E_11cy(i-1);
        else
            Ey = E_22cy(i-1);
        end
    end

    if abs(Sigma) > abs(Ey)
        fprintf('[FAILED]')
    else
        fprintf('[n_f = %.3f] ',abs(Ey/Sigma))
    end
end

```

```

    end
    fprintf('Layer %g = %.3e Pa %s\n',i-1,abs(Sigma),mode)
end
%% Main Functions

function [coords,E_11e,x_2c,H_33c] = sandwich(thickness,chord,theta,E_11,E_22,G_12,nu_12)
    nLayer = length(thickness);

    % get equivalent E_11
    nu_21 = nu_12.*E_22./E_11;
    E_11e = zeros(nLayer,1);
    R = [1,0,0;0,1,0;0,0,2];
    for i = 1:nLayer
        Q = [E_11(i)/(1-nu_12(i)*nu_21(i)),nu_21(i)*E_11(i)/(1-nu_12(i)*nu_21(i)),0;...
            nu_12(i)*E_22(i)/(1-nu_12(i)*nu_21(i)),E_22(i)/(1-nu_12(i)*nu_21(i)),0;...
            0,0,G_12(i)];

        T = [cos(theta(i))^2,sin(theta(i))^2,2*sin(theta(i))*cos(theta(i));...
            sin(theta(i))^2,cos(theta(i))^2,-2*sin(theta(i))*cos(theta(i));...
            -sin(theta(i))*cos(theta(i)),sin(theta(i))*cos(theta(i)),cos(theta(i))^2-sin(theta(i))^2];

        Sbar = inv(T\Q*R*T/R);
        E_11e(i) = 1/Sbar(1);
    end

    t_total = sum(thickness);
    %    A_total = chord.*thickness

    x_2ref = t_total/2; % location of middle
    coords = zeros(nLayer+1,1);

    for i = 1:nLayer
        coords(i+1) = coords(i)+thickness(i);
    end
    coords=coords-x_2ref; % get it into central reference frame

    x_2clayer = (coords(1:end-1)+coords(2:end))/2;
    x_2c = sum(x_2clayer.*thickness.*chord.*E_11e)/sum(thickness.*chord.*E_11e);

    H_33c = sum(chord.*E_11e.*((coords(2:end)-x_2c).^3-(coords(1:end-1)-x_2c).^3)/3);

    %    x_2c = x_2c-x_2ref;

end

%% Supporting Functions

function cfigure(winsize) % version two! :D
    screensize = get(groot,'Screensize');
    set(figure,'position',[screensize(3:4).*(1-winsize)/2,screensize(3:4).*winsize])
end

function savefigs(ext)

```

```

    if isfolder('Figures') == 0
        mkdir Figures
    end

    for i = 1:length(findobj('type','figure'))
        saveas(ffigure(i),fullfile(pwd,'Figures',num2str(i)),ext)
    end
end

```

6.3 Code Output

```
K3 =      @(x1,H33)1/H33*(IIP2(x1)+C1*x1+C2)
```

```

[n_f = 9.478]
Layer 1 = 1.455e+08 Pa (T)
[n_f = 2.412]
Layer 2 = 1.144e+07 Pa (T)
[n_f = 2.419]
Layer 3 = 1.140e+07 Pa (T)
[n_f = 2.630]
Layer 4 = 1.049e+07 Pa (T)
[n_f = 2.433]
Layer 5 = 1.133e+07 Pa (T)
[n_f = 2.441]
Layer 6 = 1.130e+07 Pa (T)
[n_f = 9.651]
Layer 7 = 1.429e+08 Pa (T)
[n_f = 2.969]
Layer 8 = 1.347e+08 Pa (T)
[n_f = 2.966]
Layer 10 = 1.348e+08 Pa (C)
[n_f = 1.639]
Layer 11 = 1.430e+08 Pa (C)
[n_f = 5.382]
Layer 12 = 9.864e+06 Pa (C)
[n_f = 5.366]
Layer 13 = 9.894e+06 Pa (C)
[n_f = 5.058]
Layer 14 = 1.050e+07 Pa (C)
[n_f = 5.334]
Layer 15 = 9.953e+06 Pa (C)
[n_f = 5.318]
Layer 16 = 9.983e+06 Pa (C)
[n_f = 1.610]
Layer 17 = 1.456e+08 Pa (C)

[Reduced Thickness = 0.819 mm]
[n_f = 8.828]
Layer 1 = 1.562e+08 Pa (T)
[n_f = 2.243]
Layer 2 = 1.230e+07 Pa (T)
[n_f = 2.246]
Layer 3 = 1.228e+07 Pa (T)
[n_f = 2.439]

```

Layer 4 = 1.131e+07 Pa (T)
[n_f = 2.253]
Layer 5 = 1.224e+07 Pa (T)
[n_f = 2.257]
Layer 6 = 1.222e+07 Pa (T)
[n_f = 8.911]
Layer 7 = 1.548e+08 Pa (T)
[n_f = 2.737]
Layer 8 = 1.461e+08 Pa (T)
[n_f = 2.736]
Layer 10 = 1.462e+08 Pa (C)
[n_f = 1.514]
Layer 11 = 1.548e+08 Pa (C)
[n_f = 4.979]
Layer 12 = 1.066e+07 Pa (C)
[n_f = 4.971]
Layer 13 = 1.068e+07 Pa (C)
[n_f = 4.693]
Layer 14 = 1.131e+07 Pa (C)
[n_f = 4.956]
Layer 15 = 1.071e+07 Pa (C)
[n_f = 4.948]
Layer 16 = 1.073e+07 Pa (C)
[n_f = 1.500]
Layer 17 = 1.563e+08 Pa (C)

7 Citations

- [1] Olivier Andre Bauchau and J. I. Craig, Structural analysis. Dordrecht [U.A.] Springer, 2009.